Chemical Thermodynamics and Thermal Analysis 7 (2022) 100070

Contents lists available at ScienceDirect

Chemical Thermodynamics and Thermal Analysis

journal homepage: www.elsevier.com/locate/ctta

DSC can be used to determine the enthalpies of formation for the 3d transition metal oxalates

Rafael Snell-Feikema, Barbara A. Reisner, Thomas C. DeVore*

Department of Chemistry and Biochemistry, James Madison University, Harrisonburg VA 22807, United States

ARTICLE INFO

Keywords:
Cobalt oxalate
Copper oxalate
Differential scanning calorimetry
Enthalpy of formation
Iron oxalate
Manganese oxalate
Nickel oxalate
Zinc oxalate

ABSTRACT

Differential scanning calorimetry has been used to measure the enthalpy of formation for manganese, iron, cobalt, nickel, copper and zinc oxalate. By adding a flameless combustion catalyst (CuO) and using scans of 2 K min^{-1} in static air, the values determined for each compound agreed to within 1% of the critically reviewed values reported previously. Confident in the approach's validity, values for metal oxalates that did not have accepted values in the compilation are also presented. This approach has the potential to measure reliable $\Delta_f H$ values for any compound where the products can be fully oxidized during the decomposition.

Introduction

The thermal decompositions of metal oxalates produces finely divided metals or metal oxides depending on the oxidation-reduction properties of the carrier gas [1–9]. Although Dollimore [4] proposed using thermodynamic calculations to select the appropriate atmosphere to needed to produce the desired product the lack of reliable thermodynamic data has limited this approach. [5] Most tables of the enthalpies of formation for the metal oxalates have missing entries and the values reported in different tables can differ by tens of kilojoules mol^{-1}. For example, Maciejewski et al. [5] found literature values ranging from -820 kJ mol^{-1} to –886 kJ mol^{-1} for the enthalpy of formation of cobalt oxalate. They presented strong evidence that these different values resulted from the failure to account for secondary chemical reactions that occurred during the decomposition of cobalt oxalate.

Evidence for secondary reactions has been reported for the thermal decomposition of several metal oxalates. Majumdar et al. [6] determined that Pt, NiO, or Fe_3O_4 catalytically oxidized CO to CO_2 during their investigation of the thermal decomposition of zinc, nickel, and iron (II) oxalate in air using Pt, Al, Al_2O_3 and Ni crucibles. Zakharov et al. [7] determined that cobalt catalytically oxidized CO in environments containing as little as 1 Pa of oxygen. Maciejewski et al. [5] found that many metal oxides were reduced to the metal by CO or H_2 under typical thermal decomposition conditions. They also established that CO disproportionation, the water gas shift reaction, and Fischer-Tropsch hydrogenation can occur in either steady-state or transient conditions. The finely divided metal produced was an effective catalyst for many of these reactions further complicating the analysis.

While it may be nearly impossible to sort out these processes to establish all of the dynamics occurring during the thermal decomposition of metal oxalates, it may still be possible to use Hess' Law to measure the enthalpy changes for these reactions. Since Hess' Law states that the enthalpy change only depends on the initial and final products and is independent of the reaction pathway, the easiest (only?) way to minimize the effect of these secondary oxidations is to use other reactions to fully oxidize the products to H_2O, CO_2, and a well-characterized metal oxide by oxidizing all reduced products (CO, C(s), H_2, the metal, etc.) produced during the decomposition process. Since slow heating rates in oxidizing atmospheres is a logical way to achieve this, the enthalpies of formation for $MC_2O_4 \cdot x\ H_2O$ where M = Mn, Fe, Co, Ni, Cu, and Zn were measured using differential scanning calorimetry (DSC) under a static air atmosphere with a scan rate of 2 K min^{-1}. The values obtained were compared to the National Bureau of Standards (NBS) values recommended by Wagman et al. [10] to determine the apparent success (or failure) of this method for each system. During the course of this investigation, it was discovered that this method did not give satisfactory results for some of the systems investigated. Since it was hypothesized that this resulted from the failure to fully oxidize the CO produced, a flameless combustion catalyst (CuO) was added to help oxidize the CO. This produced agreement between the measured and available critically reviewed enthalpies of formation to within approximately one per cent for the systems investigated.

* Corresponding author.
E-mail address: devoretc@jmu.edu (T.C. DeVore).

https://doi.org/10.1016/j.ctta.2022.100070
Received 6 April 2022; Received in revised form 14 June 2022; Accepted 20 June 2022

Experimental

With the exception of CuC_2O_4 that was purchased from Avocado Research Chemicals Ltd., all compounds were synthesized following procedures reported previously [1–9,11–24]. Adding 50.0 ml of a 1 M solution of the metal salt (chloride or nitrate) to 50 ml of 1 M $Na_2C_2O_4$ usually formed a precipitate of the metal oxalate shortly after the solutions were mixed at room temperature. The $MnC_2O_4{\cdot}3\ H_2O$ produced by mixing solutions of $MnCl_2$ and $Na_2C_2O_4$ at room temperature was converted to α-$MnC_2O_4{\cdot}2\ H_2O$ by boiling a suspension of $MnC_2O_4{\cdot}3\ H_2O$ in 50 ml of deionized water for 30 min as reported previously [11–13]. All precipitates were vacuum-filtered, washed with deionized water, and air dried for at least 24 h prior to use. FTIR and thermogravimetry (TG) were used to confirm the identity of the metal oxalate. The CuO added as a flameless combustion catalyst was prepared by placing CuC_2O_4 in an alumina container and heating it to 750 K in air for 60 min. Powder x-ray diffraction (pXRD) confirmed that this formed CuO.

Thermal gravimetric data were collected using a Mettler-Toledo TGA/stg 851[e]. All experiments were done using sample sizes between 5 and 10 mg in uncapped 70 μl alumina crucibles in atmospheres of 50 $cm^3\ min^{-1}$ flowing nitrogen or air at heating rates of 2 or 10 K min^{-1}. Mass loss measurements were corrected for buoyancy effects by subtracting the mass changes observed for an empty alumina crucible collected using the same experimental conditions. Although the sDTA were calibrated with high purity In and Zn, these measurements were only used to indicate changes in the heat flow as the carrier gas was changed. No quantitative measurements were made from sDTA and this information was not used to determine enthalpies of reaction.

Differential Scanning Calorimeter (DSC) measurements were obtained in static air at a heating rate of 2 K min^{-1} using a Mettler Toledo DSC822[e]. Carefully weighed samples (5 to 10 mg) were placed in aluminum pans, an Al top was pressure sealed to the pan, and a small hole was punched in the top to allow interaction with the atmosphere. Samples were collected with and without three (3) to four (4) mg of a flameless combustion catalyst (CuO) to determine if the gaseous decomposition products were completely oxidized during the decomposition in static air. While no change in the heat released was observed for the manganese, iron, or cobalt oxalates, increased heat release was observed for the nickel, copper and zinc oxalates. Three to five samples with different masses were heated from 298 K to 775 K using a heating rate of 2 K min^{-1} with an empty aluminum pan serving as the reference to establish the reproducibility of the measurements. The enthalpy of reaction was determined in Joules per gram (J g^{-1}) using the software in the system. A linear baseline correction was first made to correct for any drift in the system and the area under the corrected curve was determined using the software in the system. An average of several independent measurements was used to determine the values reported. The DSC was calibrated by measuring the melting points and enthalpies of fusion for high purity In, Sn, Pb, and Zn.

Since the identity of the metal oxide is needed to determine the enthalpies of formation, pXRD was done to identify the metal oxides produced during the reactions in static air. Approximately 1 gram of the metal oxalate was placed in an alumina boat and slowly heated to 775 K and then cooled in air in a tube furnace. These samples were ground in an agate mortar and pestle and mounted on a low background silicon well plate sample stage for pXRD analysis. PXRD were collected using Cu Kα radiation on a PANalytical X'Pert PRO MPD θ-θ Diffractometer equipped with an X'Celerator detector. Data were collected between 10 and 70° 2θ with a step size of 0.03° and a soak time of 25 s. The crystalline phases detected in these diffraction patterns have been identified using the ICDD PDF-2 database [25].

Results and discussion

The attenuated total reflectance - FTIR (ATR-FTIR) spectra observed for the precipitates obtained by mixing the solutions of the metal salt with a solution of sodium oxalate for each compound are presented in Fig. 1. The strong IR bands between 1700 cm^{-1} and 1200 cm^{-1} are characteristic IR bands for the oxalate ion [11,26,27]. As shown in the Fig. 1, the IR spectra for all of the compounds with n = 2 are nearly identical in this region indicating that the interactions between the metal and the oxalate are similar for these compounds. The TG for each compound presented below matched those reported previously using similar conditions and helped confirm the identity of the compound [1–9,12–24]. The observed mass losses in the dehydration region were used to establish the numbers of waters of hydration using the methods presented in Appendix 1. The total mass loss for each compound was consistent with the decomposition of one oxalate per formula unit and was used to determine the composition of the metal containing residues. These results are presented in more detail below and the procedure used to determine this is shown in Appendix 2.

Manganese oxalate

Three manganese (II) oxalate hydrates, α-$MnC_2O_4{\cdot}2\ H_2O$, γ-$MnC_2O_4{\cdot}\ 2\ H_2O$, and $MnC_2O_4{\cdot}3\ H_2O$, have been identified previously [11–13]. Donkova and Mehandjiev [13] used TG, DTA, and DSC to investigate the decomposition of α-$MnC_2O_4{\cdot}2\ H_2O$ and $MnC_2O_4{\cdot}3\ H_2O$. They reported that α-$MnC_2O_4{\cdot}2\ H_2O$ lost the water of hydration in one step with $\Delta_{hyd}H$ = 86 kJ mol^{-1} in agreement with the value of ~ 89 kJ mol^{-1} reported by Shan et al. [14] They found that $MnC_2O_4{\cdot}3\ H_2O$ lost the waters of hydration in three steps with a total $\Delta_{hyd}H$ = 132 kJ mol^{-1}. [13] $\Delta_{rxn}H$ was not determined for the decomposition of the oxalate. Mohamed et al. [8] investigated the decomposition of anhydrous manganese oxalate in several atmospheres. In nitrogen, the decomposition produced MnO and perhaps a small amount of Mn_2O_3 with $\Delta_{dec}H$ = 88 kJ mol^{-1} while the decomposition in air produced a mixture of Mn_3O_4 and Mn_2O_3 with $\Delta_{dec}H$ = -111 kJ mol^{-1}. [8] Wagman et al. [10] recommended values of -1028.8, -1628.4, and -1920.9 kJ mol^{-1} for Δ_fH of crystalline MnC_2O_4, α-$MnC_2O_4{\cdot}2\ H_2O$, and $MnC_2O_4{\cdot}3\ H_2O$, respectively. These values gave calculated values for $\Delta_{hyd}H$ of 116 kJ mol^{-1} and 166 kJ $mole^{-1}$ for the complete loss of water from $MnC_2O_4{\cdot}2\ H_2O$, and $MnC_2O_4{\cdot}3\ H_2O$. The value calculated for $\Delta_{dec}H$ in air using this data assuming complete combustion to form Mn_2O_3 was -238 kJ mol^{-1}.

The TG/ SDTA for $MnC_2O_4{\cdot}3\ H_2O$ and for α-$MnC_2O_4{\cdot}2\ H_2O$ collected at 10 K min^{-1} in flowing nitrogen and in flowing air are presented in Figs. 2 and 3, respectively. The mass loss for the removal of the waters of hydration observed between 340 K and 440 K showed no obvious dependence on the carrier gas for either compound. The observed mass loss for the dehydration of $MnC_2O_4{\cdot}3\ H_2O$ (25.6%) was less that the theoretical value (27.4%) and corresponded to the loss of ~ 2.8 water molecules per formula unit. While this could indicate that some water was retained in the lattice at 440 K, it is more likely that the missing water was lost in handling since the TG indicated that water can be lost at room temperature. The mass loss observed for α-$MnC_2O_4{\cdot}2\ H_2O$ (19.8%) was also slightly less than the theoretical value of 20.1%. This corresponded to the loss of ~1.98 moles of water/ formula unit. The procedure used to determine the chemical formulas from this data is presented in Appendix 1.

As shown in Figs. 2 and 3, the decomposition occurred at lower temperatures and the total mass loss was less for the thermal decomposition of either compound in air. The onset and peak temperatures observed in flowing nitrogen from this data and the values observed in static air from the DSC are given in Table 1. The decreased decomposition temperature indicated that the oxygen in the carrier gas was taking an active part in the decomposition. While the decomposition was endothermic in nitrogen, it changed to exothermic in air indicating that the oxygen was oxidizing the products during the decomposition. If the residue only contained manganese and oxygen, the average composition can be determined from the observed TG as shown in the Appendix 1. The residue in nitrogen was 36.85% of the initial mass for $MnC_2O_4{\cdot}\ 3\ H_2O$. Assuming this compound was actually $MnC_2O_4{\cdot}2.8\ H_2O$ as in-

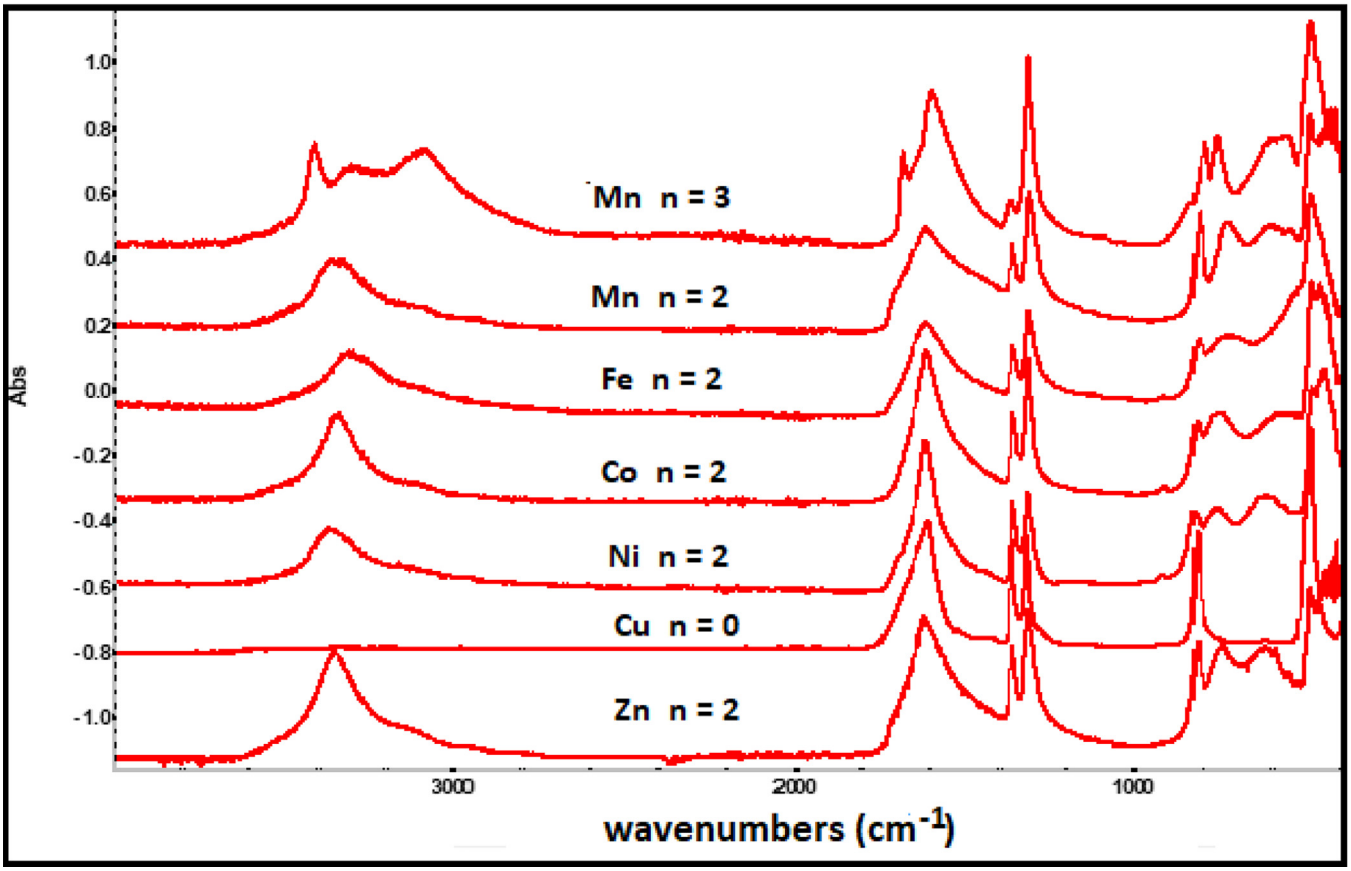

Fig. 1. The ATR-FTIR of the $MC_2O_4 \cdot n\ H_2O$ used in this investigation. All spectra were obtained using 32 scans at 4 cm^{-1} resolution. The M and n values for each compound are given in the figure.

Table 1
The onset temperatures (T_{Onset}) and the peak temperatures (T_{Peak}) in Kelvin determined for the thermal dehydration and the thermal decomposition of the metal oxalate hydrates in static air and in flowing nitrogen.

		Dehydration		Decomposition	
Compound	Atmosphere	T_{Onset}	T_{Peak}	T_{Onset}	T_{Peak}
$MnC_2O_4 \cdot 3\ H_2O$	Air	340	365	495	545
$MnC_2O_4 \cdot 3\ H_2O$	N_2	340	365	640	690
$MnC_2O_4 \cdot 2\ H_2O$	Air	380	405	510	550
$MnC_2O_4 \cdot 2\ H_2O$	N_2	385	415	640	670
$FeC_2O_4 \cdot 2\ H_2O$	Air	420	465	450	500
$FeC_2O_4 \cdot 2\ H_2O$	N_2	415	450	630	660
$CoC_2O_4 \cdot 2\ H_2O$	Air	420	455	515	545
$CoC_2O_4 \cdot 2\ H_2O$	N_2	420	450	630	650
$NiC_2O_4 \cdot 2\ H_2O$	Air	460	515	575	615
$NiC_2O_4 \cdot 2\ H_2O$	N_2	460	495	590	640
CuC_2O_4	Air	—	—	500	555
CuC_2O_4	N_2	—	—	540	560
$ZnC_2O_4 \cdot 2\ H_2O$	Air	390	435	610	655
$ZnC_2O_4 \cdot 2\ H_2O$	N_2	385	415	630	665

dicate by the measurements for the water loss, the solid produced was $MnO_{1.02}$ in agreement with the conclusion reported by Mohamed et al. [8]. A formula of $MnO_{1.71}$ was obtained from the observed mass loss of 42.56% in air. This value is slightly more oxygen rich than the composition of $MnO_{1.6}$ proposed by Ziki et al. [15]. The observed mass of the residue (39.74%) from the decomposition of α-$MnC_2O_4 \cdot 2\ H_2O$ in oxygen indicated a formula of $MnO_{1.67}$ assuming the residue only contained manganese and oxygen. The pXRD obtained by heating $MnC_2O_4 \cdot 3\ H_2O$ to 775 K in static air is shown in Fig. 4. All of the strong diffractions matched the pattern for Bixbyite (Mn_2O_3) (PDF-2 00-041-1442). There were a few minor diffractions that did not correspond to any feature in this pattern. While a complete pattern of this phase was not obtained, these features matched the stronger features of pyroluside (MnO_2) (PDF-2 00-012-0716). Our hypothesis is that while Mn_2O_3 was produced during the thermal decomposition in air, this product can be slowly oxidized to form MnO_2 with the final composition determined from TG reflecting the extent of this oxidation. This model provided an explanation for the different final compositions reported from TG data since the final compound ratios is variable and determined by the experimental conditions in the reaction zone.

The DSC's observed for both compounds in static air are shown in Fig. 5. There were no obvious differences for samples done with or

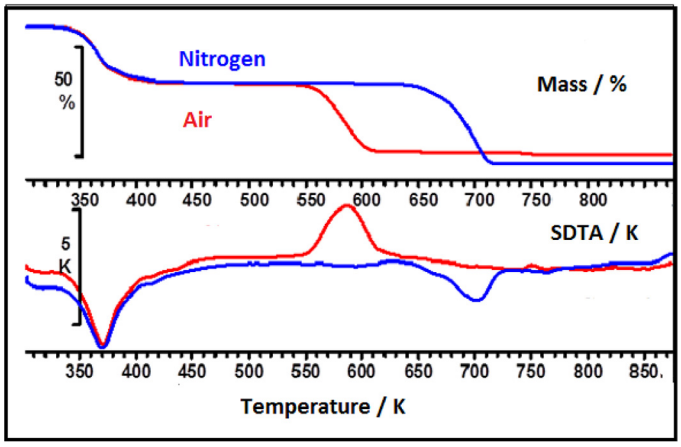

Fig. 2. The TGA and SDTA for 5 mg samples of $MnC_2O_4 \cdot 3\ H_2O$ heated in flowing nitrogen and in flowing air at 10 K min^{-1}.

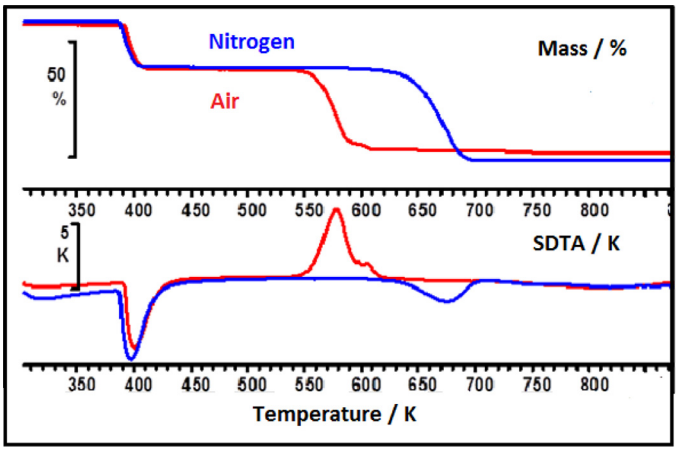

Fig. 3. The TGA and sDTA for 5 mg samples of $MnC_2O_4 \cdot 2\ H_2O$ heated in flowing nitrogen and in flowing air at 10 K min^{-1}.

without added CuO indicating that the gaseous products were oxidized by the oxygen in the carrier gas during the decomposition of these compounds. The values determined for the enthalpy of dehydration, 111 kJ mol^{-1} for α-$MnC_2O_4 \cdot 2\ H_2O$ and 155 kJ mol^{-1} for $MnC_2O_4 \cdot 3\ H_2O$ were consistent with the values calculated using the data tabulated by Wagman et al. [10] but were ~ 25 kJ mol^{-1} larger than the values reported by Shan et al. [14]. The value determined for $\Delta_{dec}H$ of MnC_2O_4 was ~ -235 kJ mol^{-1}. Assuming that the thermal decomposition initially formed Mn_2O_3, the enthalpy of reactions measured based on reactions (1) and (2)

$$MnC_2O_4 nH_2O \Leftrightarrow MnC_2O_4 + nH_2O \quad (1)$$

$$MnC_2O_4 + 3/4\ O_2 \Leftrightarrow {}^1/_2 Mn_2O_3 + 2CO_2 \quad (2)$$

gave values average values for $\Delta_f H$ of -1032, - 1625, and -1912 kJ mol^{-1} for MnC_2O_4, α-$MnC_2O_4 \cdot 2\ H_2O$, and $MnC_2O_4 \cdot 3\ H_2O$, respectively using the enthalpy values for the products given in Table 2. The method used to do these calculations is illustrated in Appendix 2. All of the values determined were within 1% of the values recommended by Wagman et al. [10]. Since any contribution from MnO_2 was not included in this calculation, the calculated enthalpies of formation may be slightly low depending on the amount of MnO_2 formed during the decomposition since the enthalpy of formation of MnO_2 per Mn is slightly larger than the value for Mn_2O_3 used. However, the agreement with the previous results showed that the method had the potential to give exact values once the products were accurately determined.

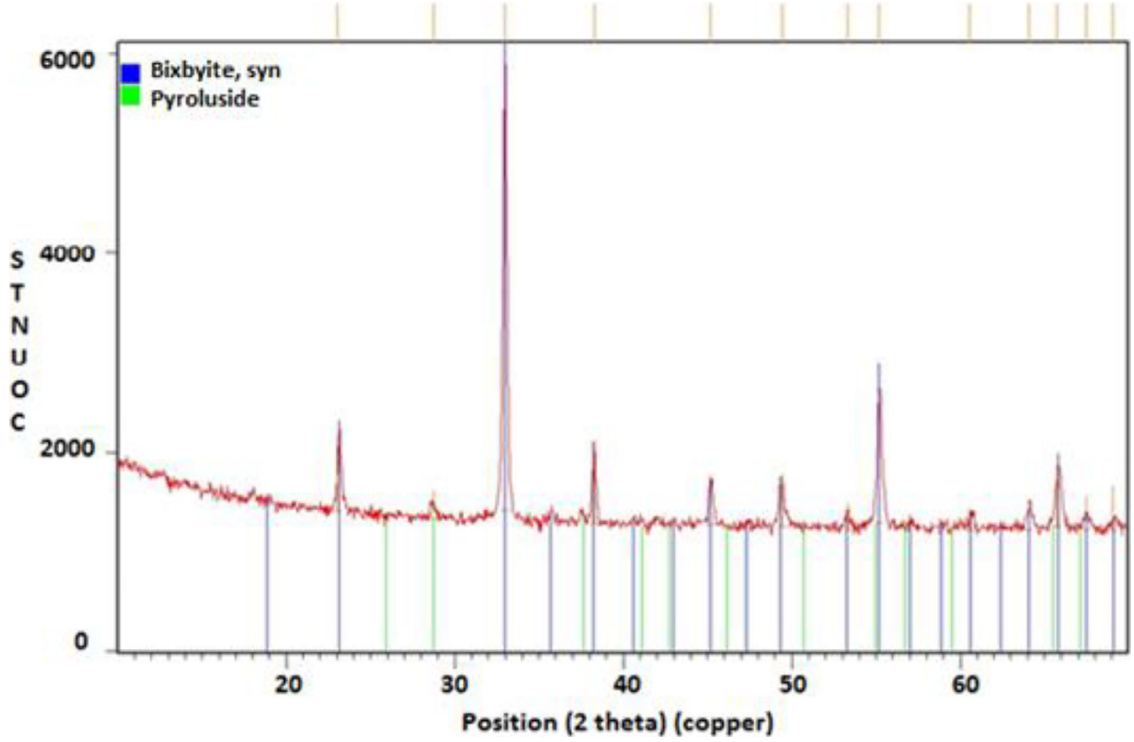

Fig. 4. The PXRD pattern observed for the decomposition products obtained by heating $MnC_2O_4 \cdot 3\ H_2O$ to 775 K in air. The principle decomposition product was identified as Bixbyite (Mn_2O_3) (PDF-2 00-041-1442). Pyroluside (MnO_2) (PDF-2 00-012-0716) could be present as a minor phase.

Table 2
Literature values from Reference 10 of the enthalpies of formation used in the calculations.

Compound	$\Delta_f H$ (kJ mol^{-1})	Compound	$\Delta_f H$ (kJ mol^{-1})
CO_2(g)	-393.509	H_2O (g)	-241.818
Mn_2O_3 (s)	-959.0	Fe_2O_3 (s)	-817.8
Co_3O_4 (s)	-891	NiO (s)	-239.7
CuO (s)	-157.3	ZnO (s)	-348.28

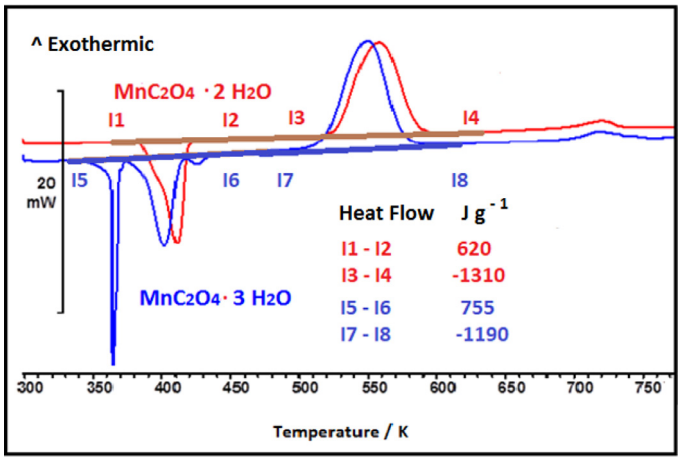

Fig. 5. DSC observed for 10 mg samples of $MnC_2O_4 \cdot 2\,H_2O$ and $MnC_2O_4 \cdot 3\,H_2O$ heated in static air at 2 K min^{-1}. The lines represent the background that was subtracted during the data analysis. The I# indicate the limits that were used to find the area of the transitions given in the figure in J g^{-1}.

Iron oxalate

Two polymorphs of $FeC_2O_4 \cdot 2\,H_2O$ have been identified [16]. While many of the previous investigations did not specify the polymorph investigated, it is reasonable to assume it was the yellow orthorhombic β form that readily precipitates from solution at room temperature. The solid product formed was very sensitive to the amount of oxygen in the carrier gas and evidence for oxidation of the residue was observed even in "pure nitrogen." [16–18]. Fe_2O_3 is the final product formed in oxygen rich environments [17–20]. Wagman et al. [10] reported a value of -1482.4 kJ mol^{-1} for $FeC_2O_4 \cdot 2\,H_2O$. They do not recommend a value for the enthalpy of formation for FeC_2O_4. Coetzee et al. [21,22] determined a value of -950 kJ mol^{-1} based on DSC measurements while Majumdar et al. [6] found a value of -921 kJ mol $^{-1}$ based on solution measurements.

The TG/ sDTA observed for β-$FeC_2O_4 \cdot 2\,H_2O$ in flowing N_2 and in flowing air are given in Fig. 6. The onset and peak temperatures observed in flowing nitrogen from this data and the values observed in static air from the DSC are given in Table 1. Two well separated endothermic transitions occurred in N_2. The mass loss for the first transition (19.9%) was slightly less than the mass loss expected from the loss of the 2 waters of hydration from $FeC_2O_4 \cdot 2\,H_2O$ (20.01%) and corresponded to the loss of 1.98 moles of water per formula unit. The total mass loss (59.05%) indicated a final composition of $FeO_{1.1}$. Since there was a clear increase in mass following the second transition, the decomposition probably produced FeO with the extra oxygen resulting from oxidation of the residue by traces of oxygen in the carrier gas. The sDTA indicated both transitions were endothermic in nitrogen.

While the dehydration did not change significantly in flowing air, the thermal decomposition moved to lower temperatures. The main effects of changing the carrier gas were that the two transitions were no longer completely separated and that the second transition was now exothermic. The total mass loss observed in air (55.1%) produced an apparent composition of the residue as $FeO_{1.54}$ indicating that Fe_2O_3 was produced under these conditions. As shown in Fig. 7, the pXRD of the compound formed in air was identified as Hematite (Fe_2O_3) in agreement with the TG results. The small exotherm at ~650 K was previously assigned as the transition from amorphous to crystalline hematite further supporting these conclusions [19].

As shown in Fig. 8, the two transitions for $FeC_2O_4 \cdot 2\,H_2O$ were not resolved in the DSC collected in static air. In order to get measurements for both peaks, a sample of $FeC_2O_4 \cdot 2\,H_2O$ was heated to 475 K in flowing nitrogen, cooled to room temperature, and used to measure the DSC for the decomposition step. The difference between the two measurements was then used to determine $\Delta_{hyd}H$. The values obtained were -282 kJ mol^{-1} for $\Delta_{dec}H$ and 100 kJ mol^{-1} for $\Delta_{hyd}H$. The measured combined enthalpy change of -182 kJ mol^{-1} did not change when CuO was added.

Assuming that the only reactions occurring were

$$FeC_2O_4 2H_2O \Leftrightarrow FeC_2O_4 + 2H_2O \quad (3)$$

$$FeC_2O_4 + 3/4O_2 \Leftrightarrow {}^1/_2Fe_2O_3 + 2CO_2 \quad (4)$$

the values determined for $\Delta_f H$ are -921 kJ mol^{-1} and -1500 kJ mol^{-1} for FeC_2O_4 and for $FeC_2O_4 \cdot 2\,H_2O$, respectively using the data in Table 2 and the procedure given in Appendix 2. While the value determined for FeC_2O_4 were consistent with the value reported by Majumdar et al., [6] the value determined for $FeC_2O_4 \cdot 2\,H_2O$ is 1.2% larger than the value recommended by Wagman et al. [10] Measurements on pure polymorphs will be needed to establish if this difference resulted from different mixtures of polymorphs in the samples or indicates an error in the measurements.

Cobalt oxalate

Values ranging from -820 kJ mol^{-1} to – 886 kJ mol^{-1} have been reported for the enthalpy of formation of CoC_2O_4 [5]. Ingier-Stocka and Rycerz [23] reported four values for $\Delta_{hyd}H$ and $\Delta_{dec}H$ based on DSC measurements using several different sets of experimental conditions. The values reported for $\Delta_f H$ from 2 K min^{-1} scans in air were -823 kJ mol^{-1} and – 1424 kJ mol^{-1}for CoC_2O_4 and $CoC_2O_4 \cdot 2\,H_2O$, respectively. Wagman et al. [10] recommended a value -851 kJ mol^{-1} for the enthalpy of formation for crystalline CoC_2O_4. They do not give a value for the hydrate. Coetzee et al. [22] reported a value of -1460 kJ mol^{-1} for $\Delta_f H$ for $CoC_2O_4 \cdot 2\,H_2O$. Maciejewski et al. [5] have shown that several secondary reactions occur during the thermal decomposition of $CoC_2O_4 \cdot 2\,H_2O$. Since the contribution of these secondary reactions will depend upon the experimental conditions, this would provide an explanation for these divergent results.

The TGA/ sDTA observed for $CoC_2O_4 \cdot 2\,H_2O$ is shown in Fig. 9. While the dehydration showed little dependence on the composition of the carrier gas, the decomposition moved to lower temperatures in air like found for the manganese and iron oxalates. The onset and peak temperatures observed in flowing nitrogen from this data and the values observed in static air from the DSC are given in Table 1. The mass loss observed for the dehydration (19.2%) indicates that ~ 1.95 moles of water were lost using the procedure given in Appendix 1. The residue contained 33.4% of the initial sample mass giving a formula of $CoO_{0.23}$ in nitrogen. Since cobalt oxalate showed a similar carrier gas dependence as the manganese and the iron oxalates, it is reasonable to assume that

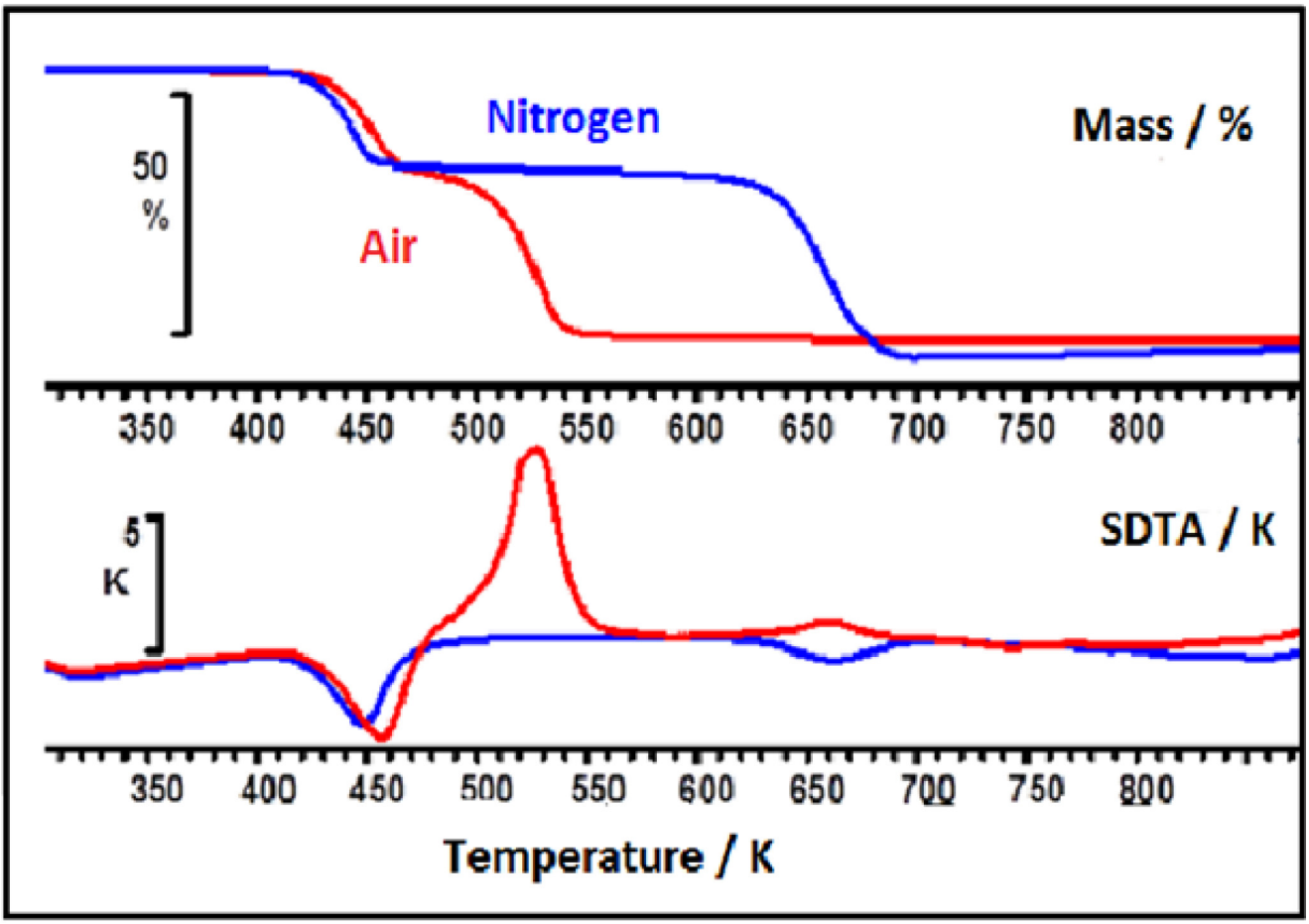

Fig. 6. The TGA and sDTA observed for 5 mg samples of $FeC_2O_4 \cdot 2\ H_2O$ heated in flowing nitrogen and in flowing air at 10 K min^{-1}.

MO, CO and CO_2 were produced initially in nitrogen atmospheres. While MnO and FeO were observed as products supporting this, the product of the cobalt system was a mixture of Co and a cobalt oxide. A secondary reaction between CoO and CO to form Co and CO_2 could explain the formation of the Co metal. The enthalpy of reaction calculated using the data from Wagman et al. [10] for this reaction is -44 kJ mol^{-1} suggesting it is favorable in this temperature range. In contrast, the reaction between MnO and CO is calculated to be +102 kJ mol^{-1} suggesting it would not occur significantly. This would explain why different products were observed for these systems. The 44.2% of the initial mass for the cobalt containing residue in air gave an apparent formula of $CoO_{1.34}$. The pXRD for a sample obtained by heating $CoC_2O_4 \cdot 2\ H_2O$ in air is shown in Fig. 10. The observed diffraction pattern matched the library pattern for Co_3O_4 (PDF-2 01-073-1701) confirming that this compound was formed from the thermal decomposition in air. The SDTA indicated that the dehydration was endothermic in both atmospheres. The slightly endothermic decomposition in nitrogen changed to exothermic in air as the products were oxidized.

The DSC in static air is shown in Fig. 11. Adding CuO to the pan did not change the observed values for either decomposition. The values obtained ($\Delta_{hyd}H$ = 104 kJ mol^{-1} and $\Delta_{dec}H$ = -225 kJ mol^{-1}) produced values of Δ_fH = -858 kJ mol^{-1} and – 1440 kJ mol^{-1} for CoC_2O_4 and $CoC_2O_4 \cdot 2\ H_2O$, respectively based on reactions (5) and (6) and using the data in Table 2 and the approach given in Appendix 2.

$$CoC_2O_4 2H_2O \Leftrightarrow CoC_2O_4 + 2H_2O \quad (5)$$

$$CoC_2O_4 + 2/3O_2 \Leftrightarrow 1/3Co_3O_4 + 2CO_2 \quad (6)$$

The value obtained for CoC_2O_4 differed by less than 1% from the recommend values given by Wagman et al. [10]

Nickel oxalate

Several values have been reported for the enthalpy of formation of NiC_2O_4. Majumdar et al. [6] proposed a value of -879 kJ mol^{-1} based on solution measurements while Zhan et al. [24] suggested a value of -885 kJ mol^{-1} based on DSC measurements. While in reasonable agreement, both values are larger than Δ_fH of -856.9 kJ mol^{-1} for crystalline NiC_2O_4 recommended by Wagman et al. [10] Zhan et al. [24] determined a value of -1465 kJ mol^{-1} for $NiC_2O_4 \cdot 2\ H_2O$ based on DSC measurements.

The TG and sDTA for $NiC_2O_4 \cdot 2\ H_2O$ are presented in Fig. 12. The onset and peak temperatures observed in flowing nitrogen from this data and the values observed in static air from the DSC are given in Table 1. Since ~2% of the mass was slowly lost after the rapid initial mass loss for several different independently prepared samples, there was more error in establishing the amount of water lost during the dehydration. The main transition showed an approximate 19.5% mass loss corresponding to the loss of 1.98 moles of water. In contrast to the manganese, iron, and cobalt oxalates, the temperature range for the decomposition step did not change significantly when air was used as the carrier gas indicating that the decomposition mechanism for $NiC_2O_4 \cdot 2\ H_2O$ was not affected by oxygen and suggesting this decomposition followed a different mechanism. In nitrogen, the residue, 32.38% of the initial sample mass, corresponded to a composition of $NiO_{0.025}$. This metal rich phase at least partially resulted from the reaction between CO and NiO as discussed above for the cobalt system since adding CuO to the DSC produced more energy

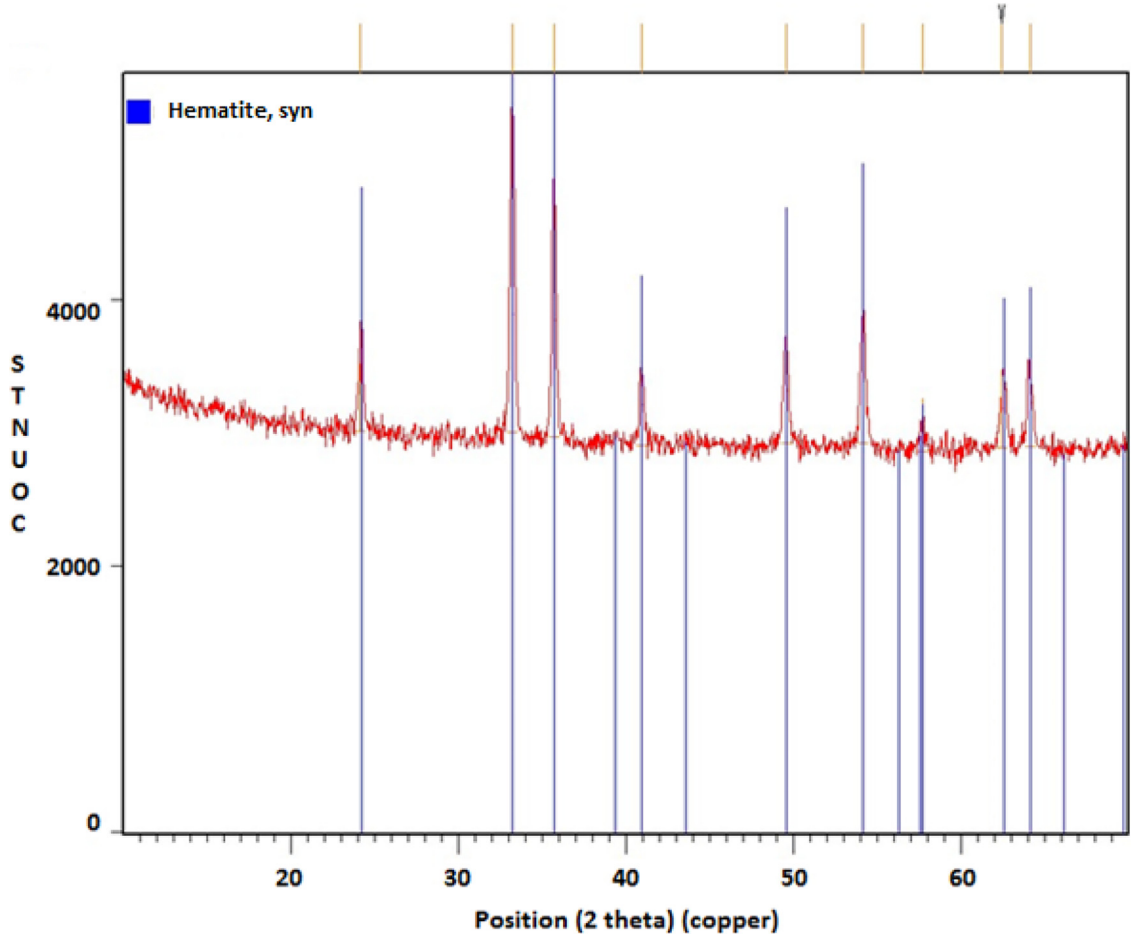

Fig. 7. A PXRD pattern observed for the decomposition product produced by heating $FeC_2O_4 \cdot 2\ H_2O$ to 775 K in static air. The product was identified as Hematite (Fe_2O_3) (PDF-2 01-076-4579).

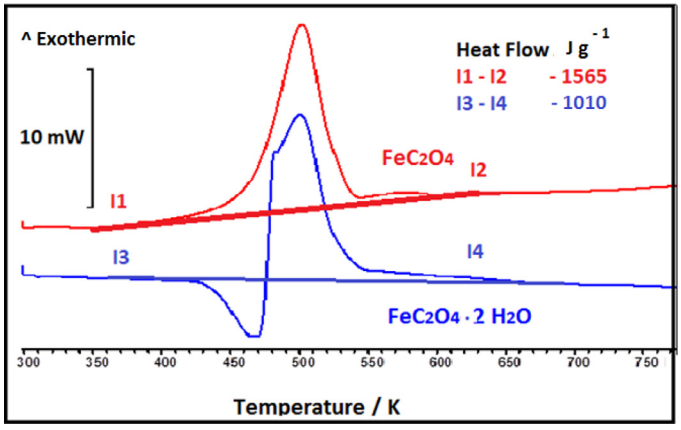

Fig. 8. DSC observed for 10 mg samples of FeC_2O_4 and $FeC_2O_4 \cdot 2\ H_2O$ in static air using a heating rate of 2 K min^{-1}. The lines represent the background that was subtracted during the data analysis. The I# indicate the limits that were used to find the area of the transitions given in the figure in J g^{-1}.

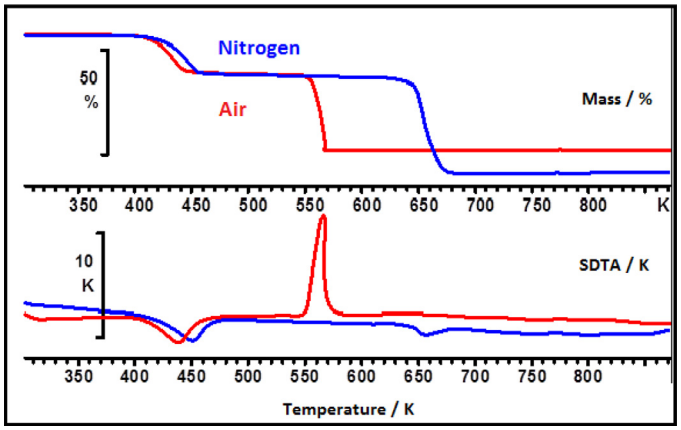

Fig. 9. The TGA and SDTA observed for 5 mg samples of $CoC_2O_4 \cdot 2\ H_2O$ heated in flowing nitrogen and in flowing air at 10 K min^{-1}.

indicating that CO was produced during the initial decomposition. Since the product was almost pure nickel, the reductive decomposition mechanism proposed by Boldyrev [28] for $Ag_2C_2O_4$ could also occur for this system. Decomposition in air produced a residue that contained 40.79% of the initial mass from the oxidation of the nickel by the oxygen in the carrier gas. This corresponds to a composition of $NiO_{0.99}$. The pXRD of the residue prepared in air shown in Fig. 13 confirmed that Burnesite (NiO) (PDF-2 01-071-1179) was produced. The sDTA indicated that the dehydration was endothermic in both atmospheres while the decomposition was slightly endothermic in nitrogen and exothermic in air from the oxidation of the products.

The DSC observed in static air is shown in Fig. 14. The value determined for $\Delta_{hyd}H$ (approximately 120 kJ mol^{-1}) was significantly larger than the value of 97 kJ mol^{-1} determined by Zhan et al. [24] or the

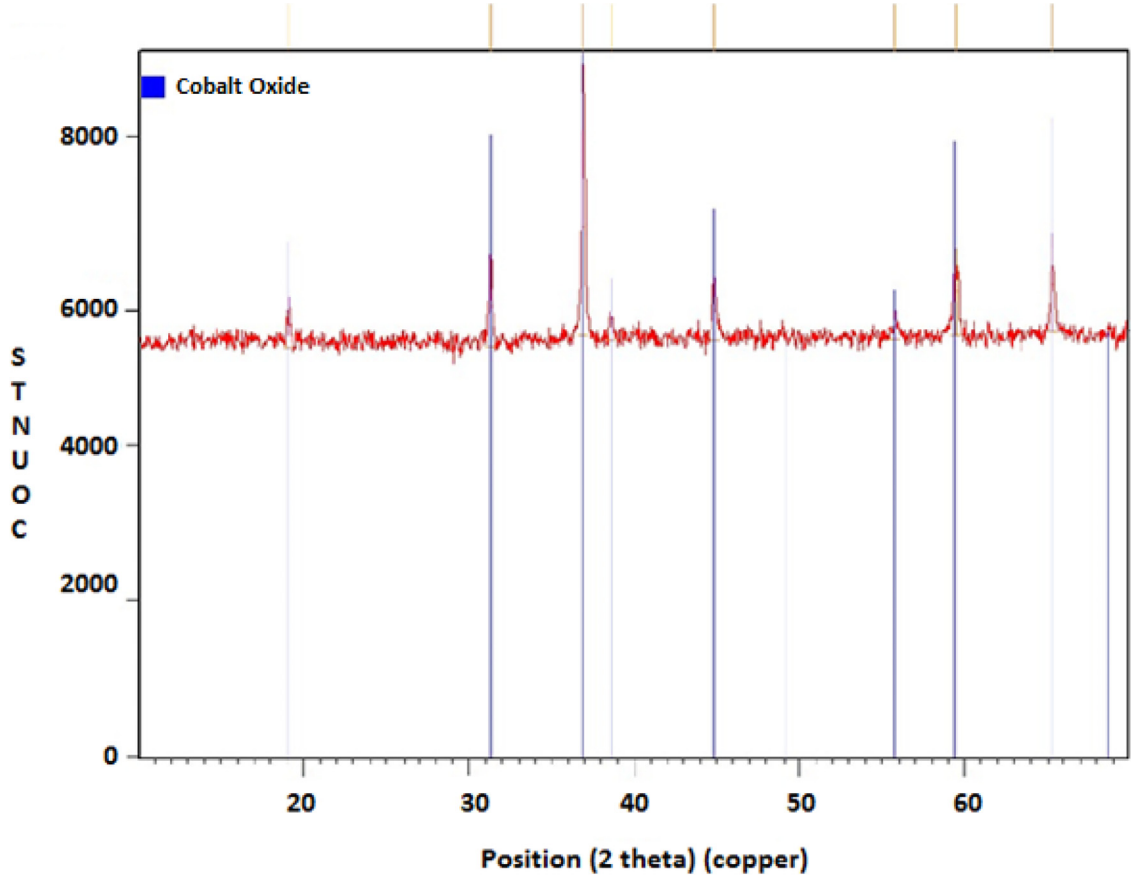

Fig. 10. The PXRD pattern observed for the decomposition product obtained by heating $CoC_2O_4 \cdot 2\,H_2O$ to 775 K in air. The product was identified as Co_3O_4 (PDF-2 01-073-1701).

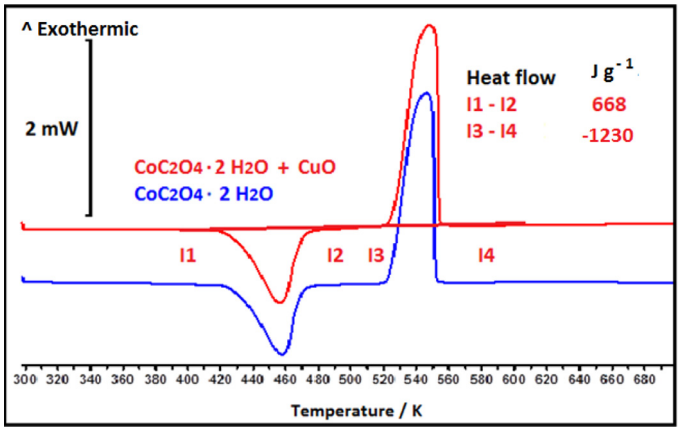

Fig. 11. The DSC observed from heating 10 mg samples of $CoC_2O_4 \cdot 2\,H_2O$ at 2 K min^{-1} in static air with and without CuO added to the cell. The lines represent the background that was subtracted during the data analysis. The I# indicate the limits that were used to find the area of the transitions given in the figure in J g^{-1}. Only the results from the sample with CuO are shown since it was the only one used to determine the enthalpy of formation.

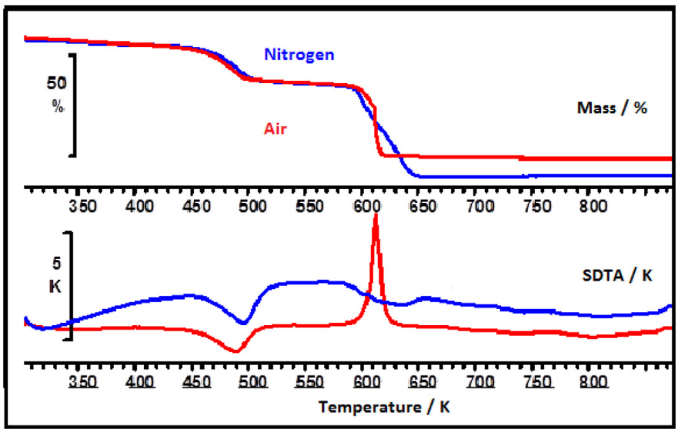

Fig. 12. The TGA and sDTA observed for 5 mg samples of $NiC_2O_4 \cdot 2\,H_2O$ heated in flowing nitrogen and in flowing air at 10 K min^{-1}.

value of 73.1 kJ mol^{-1} reported by Mohamed et al. [6]. The value of $\Delta_{dec}H$ changed from -157 kJ mol^{-1} with no CuO to -175 kJ mol^{-1} when CuO was added. The likely cause for this increase was the catalytic oxidation of the CO to CO_2 over the CuO indicating that CO was formed during the initial decomposition. The value with CuO added was used to determine Δ_fH using the data in Table 2 following the procedure given in Appendix 2 assuming the net reactions were

$$NiC_2O_4 2H_2O \Leftrightarrow NiC_2O_4 + 2H_2O \quad (7)$$

$$NiC_2O_4 + {}^1/_2O_2 \Leftrightarrow NiO + 2CO_2 \quad (8)$$

The values determined for Δ_fH were -855 kJ mol^{-1} and – 1463 kJ mol^{-1} for NiC_2O_4 and $NiC_2O_4 \cdot 2\,H_2O$, respectively. These values agree well with the value of -856 kJ mol^{-1} recommended for crystalline

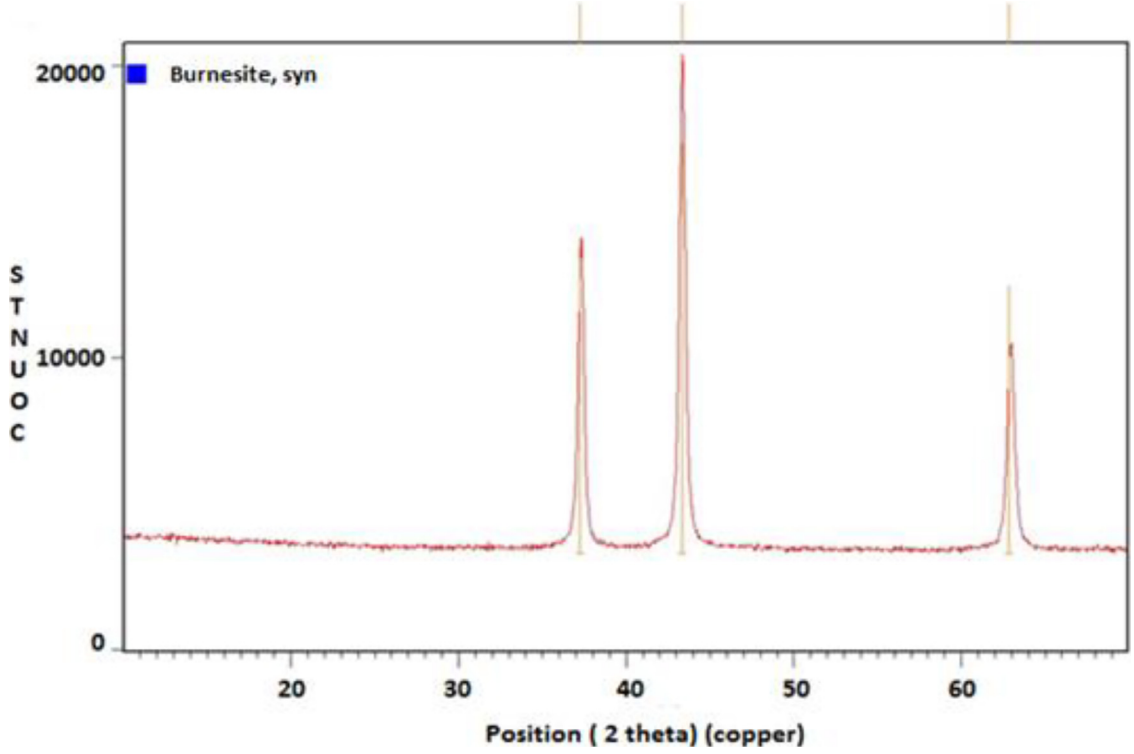

Fig. 13. The PXRD pattern observed for the decomposition product obtained by heating $NiC_2O_4 \cdot 2\,H_2O$ to 775 K in static air. The product was identified as Burnesite (NiO) (PDF-2 01-071-1179).

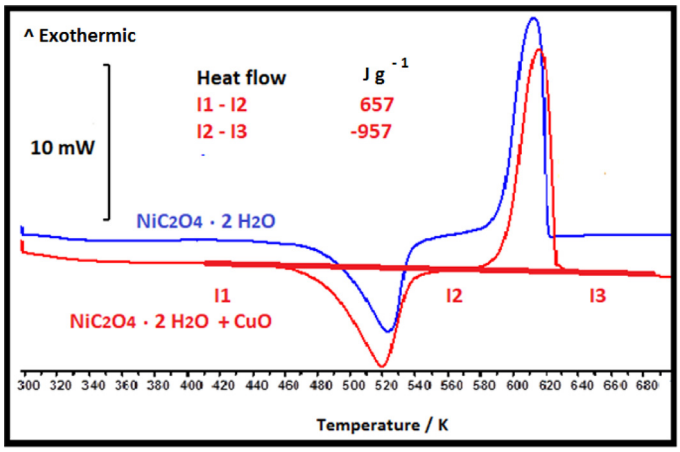

Fig. 14. The DSC observed for 10 mg samples of $NiC_2O_4 \cdot 2\,H_2O$ heated in static air at 2 K min^{-1} with and without CuO added to the cell. The lines represent the background that was subtracted during the data analysis. The I# indicate the limits that were used to find the area of the transitions given in the figure in J g^{-1}. Only the sample with CuO is shown since that was the only one used to determine the enthalpy of formation.

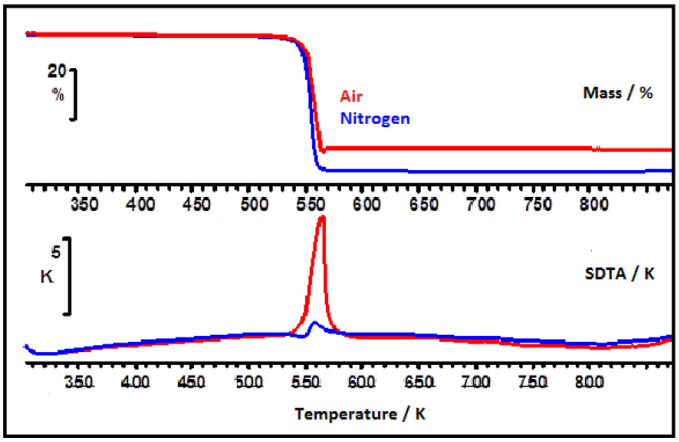

Fig. 15. The TGA and sDTA observed by heating 5 mg samples of CuC_2O_4 in flowing nitrogen and in flowing air at 10 K min^{-1}.

NiC_2O_4 by Wagman et al.[10] and the value of -1465 kJ mol^{-1} determined for $NiC_2O_4 \cdot 2\,H_2O$ by Zhan et al. [24].

Copper oxalate

The complexities observed for the thermal decomposition of copper oxalate have been discussed in detail by Lamprecht et al. [9]. Depending on the experimental conditions used, from secondary reactions with the carrier gas can produce Cu, Cu_2O and/ or CuO as the products of this decomposition. They determined $\Delta_f H$ was -751.3 kJ mol^{-1} by measuring $\Delta_{rxn} H$ in oxygen. [9]. Wagman et al. [10] do not recommend a value for crystalline CuC_2O_4.

As shown in Fig. 15, changing the carrier gas from nitrogen to air did not change the decomposition temperature range significantly indicating the decomposition was not affected by oxygen. The onset and peak temperatures observed in flowing nitrogen from this data and the values observed in static air from the DSC are given in Table 1. The 56.27% total mass loss observed for the thermal decomposition of CuC_2O_4 in N_2 corresponded to a residue composition of $CuO_{0.17}$ in agreement with the conclusions reached by Lamprecht et al. [9]. The similar results found for the nickel and copper oxalates indicate they have similar decomposition processes. The 43.54% mass loss observed in air corresponded to a composition of CuO. The pXRD shown in Fig. 16 indicated the residue produced in air was Tenorite (CuO) (PDF-2 00-048-1548) in agreement

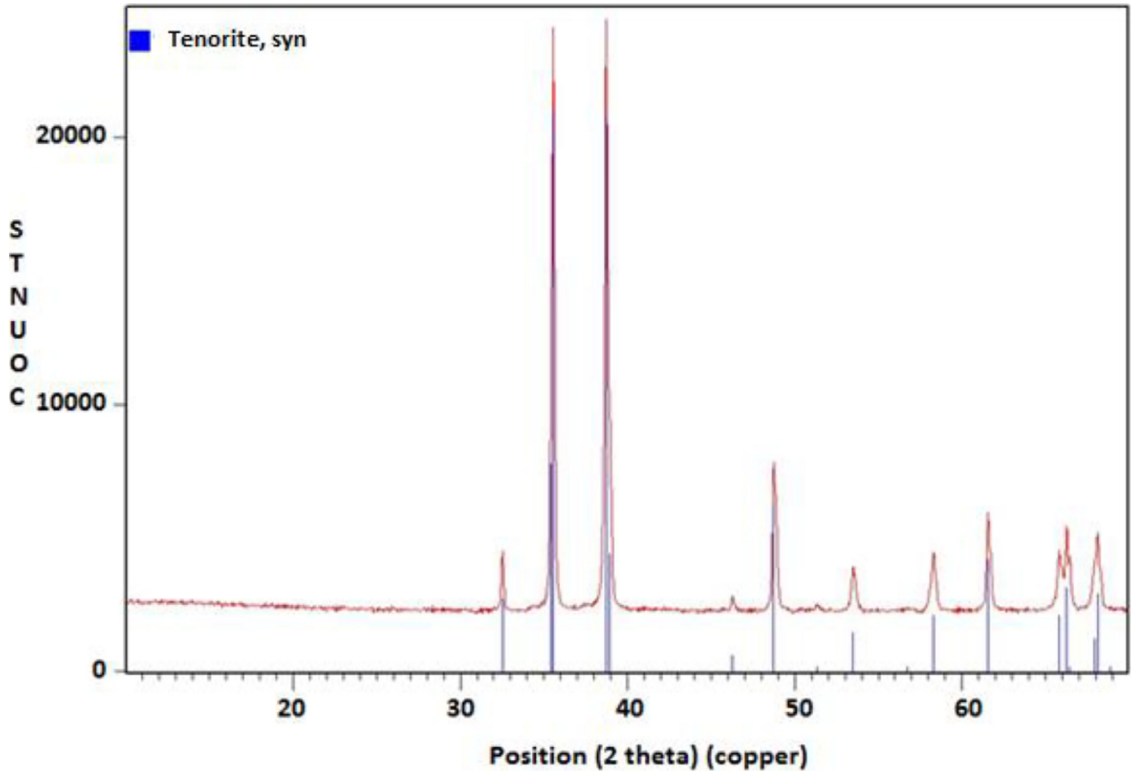

Fig. 16. The PXRD pattern observed for the decomposition product observed after heating CuC_2O_4 to 775 K in static air. The product was identified as Tenorite (CuO) (PDF-2 00-048-1548).

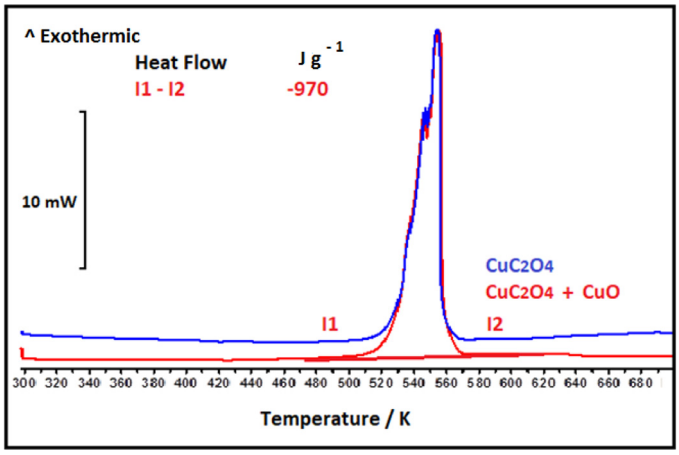

Fig. 17. The DSC obtained by heating 10 mg samples of CuC_2O_4 in static air at 2 K min^{-1} with and without CuO added to the cell. The lines represent the background that was subtracted during the data analysis. The I# indicate the limits that were used to find the area of the transitions given in the figure in J g^{-1}. Only the result from the sample with CuO is shown since it was the only one used to determine the enthalpy of formation.

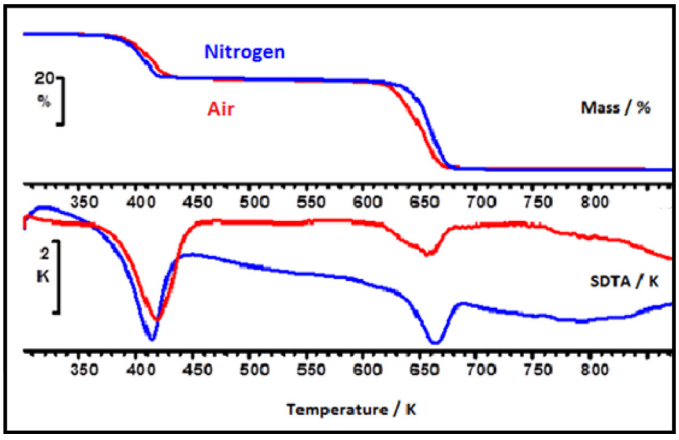

Fig. 18. The TGA and sDTA observed for 5 mg samples of $ZnC_2O_4 \cdot 2H_2O$ heated in flowing nitrogen and in flowing air at 10 K min^{-1}.

with the TG results. While the sDTA indicated this decomposition was exothermic in both atmospheres as reported previously [9], it was much more exothermic in air as the products are oxidized.

As shown in Fig. 17, the DSC indicated that the decomposition in static air was a multi-step process. The SDTA in nitrogen suggested there could be at least two steps involved in the thermal decomposition of CuC_2O_4 since it indicated there was a small weak endothermic process followed by a slightly stronger exothermic process. The initial reaction could be from a slightly endothermic reaction such as

$$CuC_2O_4 \Leftrightarrow CuO + CO + CO_2 \quad (9)$$

Since the enthalpy of formation for CO_2 is approximately 35 kJ mol^{-1} more exothermic than the sum of the enthalpies of formation of CuO and CO, the exothermic reaction in nitrogen could be from

$$CuC_2O_4 \Leftrightarrow Cu + 2CO_2 \quad (10)$$

or

$$CuO + CO \Leftrightarrow Cu + CO_2 \quad (11)$$

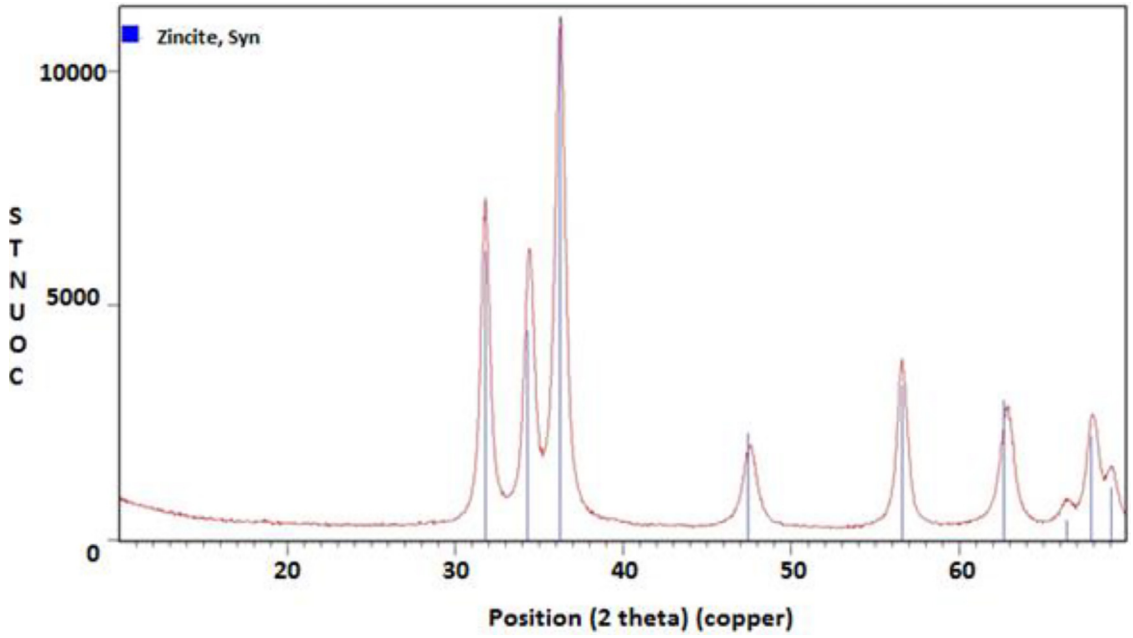

Fig. 19. The PXRD pattern observed for the decomposition product formed by heating $ZnC_2O_4 \cdot 2\ H_2O$ to 775 K in static air. The product was identified as Zincite (ZnO) (PDF-2 01-071-3830).

Adding oxygen to the carrier gas could produce secondary reaction between Cu and O_2 to form CuO giving an additional step to the decomposition and/or increase the amount of Reaction 11 occurring producing the extra decomposition steps indicated in the DSC.

$\Delta_{dec}H$ increased from -143 kJ mol^{-1} to -182 kJ mol^{-1} when CuO was added to the pan supporting the conclusion from Reaction 9 that CO was produced in the initial reaction. Assuming the **net** reaction occurring was

$$CuC_2O_4 + {}^1/_2O \Leftrightarrow CuO + 2CO_2 \quad (12)$$

and using the data in Table 2 and the procedure in Appendix 2, Δ_fH of CuC_2O_4 is calculated to be -762 kJ/ mol. This is ~ 1.5% larger than the value determined by Lamprecht et al. [9]. This difference is attributed to the more efficient oxidation of the CO formed during the decomposition by adding CuO to the cell.

Zinc oxalate

Majumdar et al. [6] suggested a value of -989 kJ mol^{-1} for Δ_fH of ZnC_2O_4. While Wagman et al. [10] do not recommend a value for ZnC_2O_4, they do recommend a value of -1564.8 kJ/mol $^{-1}$ for $ZnC_2O_4 \cdot 2\ H_2O$.

The TGA collected in air was nearly identical to the one collected in nitrogen as shown in Fig. 18. The onset and peak temperatures observed in flowing nitrogen from this data and the values observed in static air from the DSC are given in Table 1. Both indicated a mass loss of 18.97% for the dehydration corresponding to the loss of 2.0 waters using the procedure in Appendix 1. The total mass loss (57.1%) indicated the solid product was ZnO in both atmospheres and the sDTA indicated that both transitions were endothermic. The pXRD shown in Fig. 19 indicated the zinc containing product was Zincite (ZnO) (PDF-2 01-071-3830) in agreement with the TG results. Since Majumdar et al. [6] calculated that this transition would be exothermic if the CO were fully oxidized, the observed endotherm indicated CO was released and not oxidized significantly in either atmosphere. The ZnO formed in nitrogen had a grey tinge suggesting that some CO disproportionation to produced CO_2 and C occurred as found by Maciejewski et al. [5] during their thorough investigation of cobalt oxalate. This grey tinge was not observed in air indicating the carbon was oxidized.

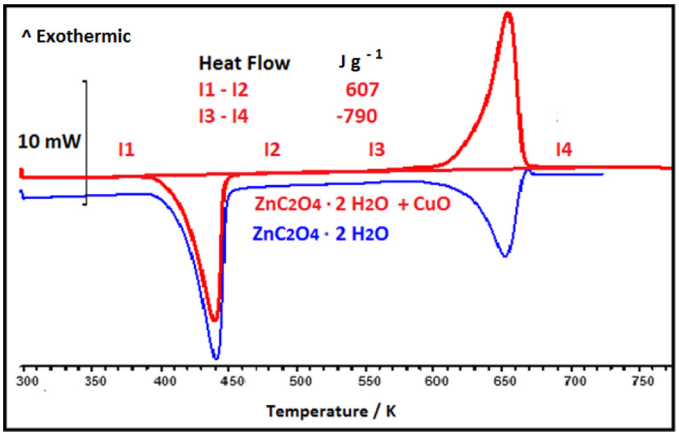

Fig. 20. DSC obtained by heating 10 mg samples of $ZnC_2O_4 \cdot 2\ H_2O$ in static air at 2 K min^{-1} with and without CuO added to the cell. The lines represent the background that was subtracted during the data analysis. The I# indicate the limits that were used to find the area of the transitions given in the figure in J g^{-1}. Only the results from the sample with CuO is shown since it was the only one used to determine the enthalpy of formation.

The DSC in static air shown in Fig. 20 confirmed that CuO oxidized the CO produced since the decomposition was endothermic without CuO and exothermic with it added. Integration of the samples with CuO gave values for $\Delta_{hyd}H$ of 115 kJ mol^{-1} and $\Delta_{dec}H$ of -150 kJ mol^{-1}. Using these values with the data in Table 2 assuming the net reactions were

$$ZnC_2O_42H_2O \Leftrightarrow ZnC_2O_4+2H_2O \quad (13)$$

$$ZnC_2O_4 + {}^1/_2O_2 \Leftrightarrow ZnO + 2CO_2 \quad (14)$$

produced Δ_fH values of -985 kJ mol^{-1} and -1580 kJ mol^{-1}, respectively. The value determined for ZnC_2O_4 was consistent with the value recommended by Majumdar et al. [6]. The value determined for $ZnC_2O_4 \cdot 2\ H_2O$ was ~ 1% larger than the value recommended by Wagman et al. [10].

Table 3
Comparison of the measured $\Delta_f H$ values in kJ mol^{-1} to those reported by Wagman et al. [10].

Compound	This Work	Wagman et al.
$MnC_2O_4 \cdot 3\ H_2O$	-1926	-1920.9
$MnC_2O_4 \cdot 2\ H_2O$	-1626	-1628.4
MnC_2O_4	-1032	-1028.8
$FeC_2O_4 \cdot 2\ H_2O$	-1500	-1482.4
FeC_2O_4	- 921	——
$CoC_2O_4 \cdot 2\ H_2O$	-1440	——
CoC_2O_4	- 858	- 851
$NiC_2O_4 \cdot 2\ H_2O$	-1463	——
NiC_2O_4	- 855	- 856.9
CuC_2O_4	- 762	——
$ZnC_2O_4 \cdot 2\ H_2O$	-1580	-1564.8
ZnC_2O_4	- 985	——

Conclusions

The composition of the carrier gas did not affect the temperature ranges or the values determined for the enthalpy of dehydration for any of the oxalates investigated. While the values determined for the enthalpy of dehydration were often larger than the values reported previously in flowing air or in flowing nitrogen, they generally agreed with the values calculated using the values tabulated by Wagman et al. [10]. Assuming these values are correct; these results indicated that measurements in static air produced more accurate enthalpies of dehydration than measurements taken in flowing gases. One possible explanation for this difference is that the flowing gases transport water droplets from the system producing a smaller measured heat change in the sample during the dehydration since these droplets do not evaporate decreasing the heat released during the dehydration. This would imply that liquid water is involved in the thermal dehydration of these compounds.

In contrast to the dehydrations, the observed temperature ranges, the enthalpies of decomposition and the products produced were very dependent on the composition of the carrier gas for the decomposition of the oxalates investigated. Manganese, iron, and cobalt oxalates decomposed at significantly lower temperatures in air than they did in nitrogen indicating that the oxygen was facilitating these decompositions. Since these metals can be oxidized above the +2 oxidation state, the first step in the decomposition could be a reaction to form a metal oxy-oxalate in oxygen atmospheres that decomposed through the loss of two molecules of CO_2. Adding CuO to the cell did not change the values observed for $\Delta_{dec}H$ for these compounds indicating there was little CO produced during the decomposition in air. In contrast, Ni, Cu, and Zn oxalates showed little temperature change when air was used as the carrier gas indicating that the carrier gas was not significantly involved in the initial decomposition mechanism. Since these metals rarely form oxidation states above +2, they were not oxidized and followed the same mechanism in both carrier gases. The magnitude of $\Delta_{dec}H$ increased when CuO was added to the cell for these compounds indicating that CO formed initially and was oxidized via a secondary reaction with the CuO. Oxidizing the CO and forming the metal oxide from reaction with oxygen in the carrier gas reduced the complexity of the system.

The enthalpies of formation determined are compared to the values tabulated by Wagman et al. [10]. in Table 3. The values generally agreed to within the uncertainty of the measurements (~1%). The main limitation of the method proposed is the assumption that the CO was completely oxidized to CO_2. If this is not true, the values calculated will be too large establishing an upper limit for the enthalpy of formation.

While these measurements produced values for $\Delta_f H$ within one percent of the most reliable values, the object of this investigation was not to produce better values for the enthalpies of formation for these transition metal oxalates. The object of this investigation was to determine if a method could be developed that minimized the effect of the secondary reactions on the measured heat flow and had the potential to produce accurate values for the enthalpy changes during these decomposition processes. The results indicated that using static air to generate oxidizing conditions and including a flameless combustion catalyst had the potential to reach this goal. Generating better values for the enthalpies of formation of these oxalates will require better characterized samples (especially for the compounds that have more than one polymorph), more duplicate measurements to minimize random errors, and adjusting the values measured at temperature to the enthalpy values at standard conditions. The results obtained here indicate that DSC using highly oxidizing conditions has the potential to determine accurate values for the enthalpies of formation if pure samples containing one polymorph can be obtained Eqs. (1)–(14).

Declaration of Competing Ineterest

None

Acknowledgements

The authors gratefully acknowledge the NSF REU (CHE-1461175), MRI (CHE-0320245), and IMR (DMR-0315345) programs.

Appendix 1. Determination of the metal oxide formula from TG date.

I. Determination of the percent mass loss.
A. The first step was to correct for buoyancy effects by subtracting the TG observed for an empty cell from the TG observed for the sample.
B. The percent mass loss was determined from the base line before the transition to the base line after the transition in the corrected TG using the software in the instrument. The values determined for the percent mass are given in the text.
II. Determination of the chemical formula from the percent mass.

This is illustrated by determining the chemical formula for the residue produced from the thermal decomposition of $MnC_2O_4 \cdot 2.8\ H_2O$ in nitrogen where the mass of the residue was 36.85%.

A. The molar mass of $MnC_2O_4 \cdot 2.8\ H_2O$ used was 193.3 g mol^{-1}.
B. The molar mass of the residue is = % mass of the residue * molar mass of compound = 0.3685 * 193.3 g mol^{-1} = 71.23 g mol^{-1}.
C. The residue contained 1 mole (54.938 g mol^{-1}) of manganese since the percent mass loss was based on the decomposition of one mole of $MnC_2O_4 \cdot 2.8\ H_2O$.
D. By difference, the residue contained a mass oxygen = mass residue – mass manganese.

Mass oxygen = 71.23 g – 54.938g = 16.3 g.

A. Moles oxygen = mass oxygen / molar mass oxygen.

Moles oxygen = 16.3 g / 16.0 g mol^{-1} = 1.02 moles.

A. Giving a formula of $MnO_{1.02}$.

Appendix 2. Determination of the Enthalpy of Formation for the metal oxalates

I. Determination of the enthalpy of reaction.

A. The DSC baseline was corrected by subtracting a line a connecting a point prior to the transition to a point after the transition as illustrated in Figs. 5, 8, 11, 14, 17 and 20.
B. The area under the curve was determined from the point prior to the transition to the point after the transition. The points used are illustrated in Figs. 5, 8, 11, 14, 17 and 20.

C. The software was used to determine the heat flow by integrating the area under the curve and dividing by the sample mass. The values determined in J g^{-1} for the average of several measurements are given in Figs. 5, 8, 11, 14, 17 and 20.
D. Multiplying the heat flow by the molar mass gave the enthalpy of reaction for the process.

Illustrating using the thermal decomposition of $MnC_2O_4 \cdot 2\ H_2O$ with a molar mass of 178.9888 g mol^{-1}.

A. The heat flow was -1310 J / g (from Fig. 4).
B. The enthalpy of Reaction = Heat flow * Molar Mass

= -1310 J / g * 178.9888 g mol^{-1} = -234 kJ mol^{-1}.
(This vale is estimated to be good to ± 5 kJ mol^{-1}).

II. Determination of the enthalpy of formation for the metal oxalate

A. This calculation requireed a balanced chemical reaction. All of the balanced chemical reactions were based on the metal oxide compositions determined from the TG and the pXRD data. They assumed that any CO formed was completely oxidized to CO_2. If this was not correct, the values calculated will be larger than the true value giving the maximum possible value.
B. By Hess' Law $\Delta_{rxn}H = \Sigma\ \Delta_fH_{products} - \Sigma\ \Delta_fH_{reactants}$.
C. Rearranging this equation and using the values in Table 2 gives the enthalpy of formation for the metal oxalate.

Illustrating using the thermal decomposition of MnC_2O_4 using the reaction

$$MnC_2O_4 + 3/4\ O_2 \Leftrightarrow {}^1/_2Mn_2O_3 + 2CO_2$$

with $\Delta_{rxn}H$ = -234 kJ mol^{-1}.
$\triangle rxnH = \sum \triangle_f H_{products} - \sum \triangle_f H_{reactants}$
$. = 1/2\ \triangle_f H_{Mn2O3} + 2\triangle_f H_{CO2} - \triangle_f H_{MnC2O4} - 3/4\triangle_f H_{O2}$
Rearranging gave
$\triangle_f H_{MnC2O4} = 1/2\triangle_f H_{Mn2O3} + 2\triangle_f H_{CO2} - 3/2\triangle_f H_{O2} - \triangle_{rxn}H.$
Plugging in the values from Table 2, gave
$\Delta_fH_{MnC2O4} = \frac{1}{2}$ * -959 + 2 * -393.509 – $\frac{3}{4}$ 0.0 – (-234) kJ mol^{-1}
= -1032 kJ mol^{-1}.

III. Determination of the enthalpy of formation of metal oxalate hydrate.

A. This calculation required a balanced chemical reaction. All of the balanced chemical reactions assumed that all of the water was removed to form the dehydrated metal oxalate.
B. By Hess' Law $\Delta_{rxn}H = \Sigma\ \Delta_fH_{products} - \Sigma\ \Delta_fH_{reactants}$.
C. Rearranging this equation and using the values in Table 2 gave the enthalpy of formation for the metal oxalate.

Illustrating for the dehydration of $MnC_2O_4 \cdot 2\ H_2O$ with $\Delta_{rxn}H$ = 111 kJ mol^{-1} and Δ_fH_{MnC2O4} = -1032 kJ mol^{-1} in Eq. (A1)

$$MnC_2O_4 \cdot 2H_2O \Leftrightarrow MnC_2O_4 + 2H_2O \quad (A1)$$

$$\triangle_{rxn}H = \sum \triangle_f H_{products} - \sum \triangle_f H_{reactants}$$

$$= \triangle_f H_{MnC2O4} + 2\triangle_f H_{H2O} - \triangle_f H_{MnC2O4-2H2O}$$

Rearranging gave

$$\triangle_f H_{MnC2O4-2H2O} = \triangle_f H_{MnC2O4} + 2\triangle_f H_{H2O} - \triangle_{rxn}H$$

Calculating with the values from Table 2, gave
$\Delta_fH_{MnC2O4-\ 2\ H2O}$ = -**1032** + 2 * -241.818 – 111 kJ mol^{-1}
= -1626 kJ mol^{-1}.

References

[1] K.V. Krishnamurty, G.M. Harris, The chemistry of metal oxalate complexes, Chem. Rev. 61 (1961) 213–246.
[2] D. Dollimore, D. Nicholson, The thermal decomposition of oxalates. Part I. The variation of surface area with the temperature of treatment in air, J. Chem. Soc. (1962) 960–965.
[3] D. Dollimore, D.L. Griffiths, D Nicholson, The thermal decomposition of oxalates. Part II. Thermogravimetric analysis of various oxalates in air and in nitrogen, J. Chem. Soc. (1963) 2617–2623.
[4] D. Dollimore, The production of metals and alloys by the decomposition of oxysalts, Thermochim. Acta 177 (1991) 59–75.
[5] M. Maciejewski, E. Ingier-Stocka, W.D. Emmerich, A. Baiker, Monitoring of the gas phase composition: a prerequisite for unraveling the mechanism of decomposition of solids. Thermal decomposition of cobalt oxalate dihydrate, J. Therm. Anal. Calorim. 60 (2000) 735–758.
[6] P. Majumdar, P. Sarjar, M. Roy Mukhopadhyay, Secondary catalytic reactions during thermal decomposition of oxalates of zinc, nickel, and iron (II), Thermochim. Acta 335 (1999) 43–53.
[7] A.N. Zakharov, A.F. Mayorova, N.S. Perov, Peculiarities on polythermic decomposition of iron, cobalt, and nickel oxalates within the pores of photonic crystals based on SiO2 in atmosphere with oxygen lack, J. Therm. Anal. Calorim. 92 (2008) 747–750.
[8] M.A. Mohamed, A.K. Galwey, S.A. Halwy, A comparative study of the thermal reactivities of some transition metal oxalates in selected atmospheres, Thermochim. Acta 429 (2005) 57–72.
[9] E. Lamprecht, G.M. Watkins, M.E. Brown, The thermal decomposition of copper (II) oxalate revisited, Thermochim. Acta 446 (2006) 91–100.
[10] D.D. Wagman, W.H. Evans, V.P. Parker, R.H. Shumm, I Halow, S.M. Bailey, K.L. Churney, R.L. Nuttall, The NBS tables of chemical thermodynamic properties: Selected values for inorganic and C_1 and C_2 organic substances, J. Phys. Chem. Ref. Data 11 (2) (1982) Supplement No.
[11] N. Mancilla, V. Caliva, M.C. D'Antonio, A.X. Gonzalez-Baro, E.J. Baran, Vibrational spectroscopic investigation of the hydrates of manganese (II) oxalate, J. Raman Spectrosc. 40 (2009) 915–920.
[12] A. Huizing, H.A.M. van Hal, W. Kiwestroo, C. Langereis, P.C. van Loosdregt, Hydrates of manganese (II) oxalates, Mater. Res. Bull. 12 (1977) 605–611.
[13] B.D. Donkova, D. Mehandjiev, Mechanism of decomposition on manganese (II) oxalate dehydrate and manganese (II) oxalate trihydrate, Thermochim. Acta 421 (2004) 141–149.
[14] H.W. Shan, D.H. Chen, W.J. Tang, Thermodynamics and thermal analysis kinetics of MC_2O_4 (M=Mn, Fe, Co, Ni, Cu, Zn), Acta Phys. Chim. Sin. 21 (2005) 1001–1005.
[15] M.I. Zaki, A.K. Nohman, Ch. Kappenstein, T.M. Wahdan, Temperature programmed characterization studies of thermochemical events occurring in course of decomposition on Mn(II) salts, J. Mater. Chem. 5 (1995) 1081–1088.
[16] A. Angermann, Topfer J, Synthesis of magnetite nanoparticles by thermal decomposition of ferrous oxalate, J. Mater. Sci. 43 (2008) 5123–5130.
[17] E.D. Macklen, Influence of atmosphere on the thermal decomposition of ferrous oxalate dehydrate, J. Inorg. Nucl. Chem. 19 (1967) 1229–1234.
[18] M. Hermanek, R. Zboril, M. Mashlan, L. Machala, O. Schneeweiss, Thermal behavior of iron (II) oxalate dehydrate in the atmosphere of its conversion gases, J. Mater. Chem. 16 (2006) 1273–1280.
[19] K. Koga, Y. Sato, Formation and transformation kinetics of amorphous iron (III) oxide during the thermally induced transformation of ferrous oxalate dehydrate in air, J. Phys. Chem. A 115 (2011) 141–151.
[20] W-J. Tang, D-H. Chen, Thermal decomposition kinetics of ferrous oxalate dehydrate, Acta Phys. Chim. Sin. 23 (2007) 605–608.
[21] A. Coetzee, D.J. Eve, M.E. Brown, Thermal analysis of some mixed metal oxalates, J. Therm. Anal. 39 (1993) 947–973.
[22] A. Coetzee, M.E. Brown, D.J. Eve, C.A. Strydom, Kinetics of the thermal dehydrations and decompositions of some mixed metal oxalates, J. Therm. Anal. 41 (1994) 357–385.
[23] E. Ingier-Stocka, L. Rycerz, Thermochemistry of the decomposition of some cobalt compounds, J. Therm. Anal. Calorim. 56 (1999) 547–552.
[24] D. Zhan, C. Cong, K. Diakite, Y. Tao, K. Zhang, Kinetics of thermal decomposition of nickel oxalate dihydrate in air, Thermochim. Acta 430 (2005) 101–105.
[25] S. Gates-Rector, T. Blanton, The powder diffraction file: a quality materials characterization database, Powder Diffr. 34 (2019) 352–360, doi:10.1017/S0885715619000812.
[26] K. Nakamoto, Infrared Spectra of Inorganic Coordination Compounds, 2nd ed., Wiley Interscience, New York, 1970.
[27] R.L. Frost, Raman spectra of natural oxalates, Anal. Chim. Acta 517 (2004) 207–214.
[28] V.V. Boldyrev, Thermal decomposition of silver oxalate, Thermochim. Acta 388 (2002) 63–90.